Scanning Speed and Powder Flow rate influence on the Properties of Laser Metal Deposition of Titanium Alloy

Rasheedat M. Mahamood [a,b,*] **and** ***Esther T. Akinlabi*** [a]

[a]*University of Johannesburg, Johannesburg, South Africa.*

University of Ilorin, Nigeria.

**Corresponding author email: mahamoodmr2009@gmail.com*

Abstract

Ti4Al4V is an important aerospace alloy because of its excellent properties that include high strength to weight ratio and corrosion resistance. In spite of these impressive properties processing titanium is very challenging which contributes to the high cost of the material. laser metal deposition, an important additive manufacturing method is an excellent alternative manufacturing process for Ti6Al4V. The economy of this manufacturing process also depends on the right combination of processing parameters. The principal aim of this study is to know the optimum processing parameters that will result in deposit with sound metallurgical bonding with the substrate with proper mechanical property and better surface finish. This will help to reduce the need for expensive secondary finishing operations using this manufacturing process. This study investigates the influence of scanning speed and the powder flow rate on the resulting properties of the deposited samples. Microstructure, Microhardness and surface finish of Ti6Al4V samples that were produced using the laser metal deposition process over a range of scanning speeds, ranging from 0.02 to 0.12 m/s and powder flow rate of ranging from 0.72 to 6.48 g/min. The

microstructure, microhardness and surface finish were characterized using the optical microscopy, Metkon hardness tester and Jenoptik surface analyzer respectively. These process parameters variations were mapped with the microstructure, the microhardness and surface roughness. The microstructures were found to change from the thick lath of basket woven to martensitic microstructure as the scanning speed and the powder flow rate were increased. The microhardness and the surface roughness were found to increase as the scanning speed and the powder flow rate was increased. It can be concluded that in order to minimize the surface roughness while maintaining a moderate microhardness value, the optimum scanning speed is about 0.63 m/s while the powder flow rate should be maintained at 2.88 g/min. The laser power and the gas flow rate should also be fixed at 3 kW and 2 l/min respectively.

Keywords: Additive Manufacturing; Mechanical Properties; Optical Microscopy; powder flow rate; Scanning speed; surface roughness

1. INTRODUCTION

Laser metal deposition process belongs to the directed energy deposition class of additive manufacturing that can produce three dimensional (3D) objects directly from the 3D computer aided design (CAD) by incrementing the material layer by layer.[1] In this process, the laser is focused on the substrate thereby creating a melt-pool on the substrate. The powder or wire material is then delivered into the melt pool causing the delivered materials to be melted and upon solidification forming a track of the deposited material that is metallurgically bounded to the substrate. Laser metal deposition process is a promising advanced manufacturing process that is

capable of reducing the buy-to-fly ratio and also capable of repairing high valued parts that were prohibitive or not repairable in the past. [2-4] Laser metal deposition process like any additive manufacturing is a tool-less manufacturing process making it an ideal alternative manufacturing process for difficult to machine materials such as titanium and its alloys.

Ti6Al4V is an important titanium alloy and it is the most commonly produced and the most widely used titanium alloy .[5] Ti6Al4V is often referred to the workhorse of the industry because of the excellent properties possessed by the alloy .[6] These properties include: high strength-to-weight ratio, excellent corrosion resistance and heat treatable .[7] The use of laser metal deposition to produce or repair high valued parts is an interesting research area because of the great potential of this manufacturing technology.[3,4,8-17] Processing parameters play an important role in the properties of the deposited parts. [11, 13, 18-24]

The aim of this study is to establish the influence of scanning speed and the powder flow rate on the evolving physical, metallurgical and mechanical properties of the deposited samples. The properties that are investigated are respectively the surface roughness, the microstructure and the microhardness. This study will help to establish the optimized processing parameter that will give optimize surface finish and better mechanical property. This will help to reduce the need for secondary finishing operation after the deposition of the part. The results are presented and discussed in detail.

2. MATERIALS AND METHOD

In this study, an experimental set-up available at the National Laser Center, CSIR, Pretoria, South Africa as shown pictorially in Figure 1 was used. [20] The experimental set-up consists of a Kuka robot that carries Nd-YAG laser and co-axial powder nozzles in its end effector. The Nd-YAG laser is of maximum power output of 4 kW with wavelength of 1.06 μm because of its suitability for processing this type of material. [25] The controlled environment chamber was improvised by using plastic wrapping, Argon gas and box that as shown in Figure 1 helps to prevent contamination of the deposited samples from the atmospheric oxygen and Nitrogen by keeping the oxygen level below 10 PPM. The laser focal length is maintained at a distance of 195 mm above the substrate and with spot size of 2 mm.

Figure 1. Experimental Set-up [20]

The substrate materials and the powder material used in this study is Ti6Al4V of 99.6 % purity. The substrate is hot rolled sheet of 70 X 70 X 5 mm in dimension. The Ti6Al4V powder is gas atomized powder. The substrate was sandblasted and washed with acetone before the deposition process. The laser power was maintained at a value of 3.0 kW and the gas flow rate at a value of 2 l/min throughout the experiments. Experimental matrix with varying scanning speed and varying powder flow rate are shown in Table 1 and Table 2 respectively.

Table 1. Experimental matrix with varying scanning speed

Sample Label	**Scanning speed (m/s)**	**Powder Flow Rate (g/min)**
A1	0.02	2.88
A2	0.04	2.88
A3	0.06	2.88
A4	0.08	2.88
A5	0.1	2.88
A6	0.12	2.88

Table 2. Experimental matrix with varying Powder flow rate

Sample Label	**Powder Flow Rate (g/min)**	**Scanning Speed (m/s)**
B1	0. 72	0.06
B2	1.44	0.06
B3	2.88	0.06
B4	4.32	0.06

B5	5.76	0.06
B6	6.48	0.06

After the deposition process, the as deposited sample was washed with acetone before the surface roughness measurements. The surface roughness of each track of the samples was measured with stylus surface analyzer by Jenoptik, equipped with Hommelmap 6.2 software. The measuring condition was in accordance with the 'BS EN ISO 4288:1998' standard. [26] Five measurements were taken on each of the samples, and the arithmetic average of the 2D roughness profiles (Ra) was recorded. The samples for the microhardness and the microstructure were then cut in the vertical direction of the deposited track so as to reveal the cross section of the samples. The cut samples were mounted in resin ground and polished following the standard metallurgical preparation of titanium and its alloys. [27] The samples for microstructural examination were etched using the Kroll's reagent and the microstructure was studied under Olympus BX51M Optical Microscopy (OP) equipped with an Olympus DP25 digital camera. The microhardness indentation were taken using a Vickers microhardness indenter with a load of 300 g and a dwelling time of 15s according to the ASTM E92 - 16 standard.[28] The distance between indentation was maintained at a distance of 15 μm. The distance of 15 μm between indentations was chosen because it is more than twice the size of indentation which is recommended by the ASTM standard.

3. RESULTS

The microstructure of the Ti6Al4V substrate is shown in Figure 2 (a). The morphology of the Ti6Al4V powder is shown in Figure 2 (b). The micrographs of the deposited samples A1, A6, B1

and B5 are shown in Figure 3 (a), 3 (b), 3 (c) and 3 (d) respectively. The micrographs showing the microstructure of samples produced at (a) scanning speed of 0.06 m/s and powder flow rate of 0.72 g/min is shown in Figure 4 (a) and that of the sample at a scanning speed of 0.06 m/s and powder flow rate of 6.48 g/min is shown in Figure 4 (b). The results of the effect of the varying scanning speed on the microhardness and the average surface roughness are presented in Table 3. The results of the influence of the powder flow rate on the microhardness and average surface roughness are presented in Table 4. The microhardness indentation produced on the sample deposited at a scanning speed of 0.04 and powder flow rate of 2.88 g/min is shown in Figure 5. The graph of the microhardness and surface roughness against the scanning speed is shown in Figure 6 (a) and the graph of microhardness and surface roughness versus powder flow rate is shown in Figure 6 (b).

Table 3. Results with varying scanning speed

Sample Label	**Scanning Speed (m/s)**	**Powder Flow Rate (g/min)**	**Microhardness (HV)**	**Surface Roughness (Ra)**
A1	0.02	2.88	330.60	5.5
A2	0.04	2.88	354.05	14.01
A3	0.06	2.88	379.05	18.09
A4	0.08	2.88	405.79	20.93
A5	0.1	2.88	442.02	22.98
A6	0.12	2.88	446.06	23.09

Table 4. Results with varying Powder flow rate

Sample Label	**Powder Flow Rate (g/min)**	**Scanning Speed (m/s)**	**Microhardness (HV)**	**Surface Roughness (Ra)**
B1	0. 72	0.06	329.89	3.60
B2	1.44	0.06	346.04	11.04
B3	2.88	0.06	379.05	16.09
B4	4.32	0.06	409.38	19.01
B5	5.76	0.06	438.90	21.76
B6	6.48	0.06	450.59	22.08

4. DISCUSSION

The microstructure of the Ti6Al4V substrate shown in Figure 2 (a) and it is characterized by beta phase in the matrix of alpha grains structure. The alpha phase is colored lighter by the etchant while the beta phase is coloured darker as shown in Figure 2 (a). This microstructure is typical of any Ti6Al4V because of the alpha and beta stabilizers contained in the alloy- aluminium and vanadium. This microstructure is what is responsible for the excellent properties of this titanium alloy and it is responsible for the highest strength-to-weight-ratio property posses by the alloy.

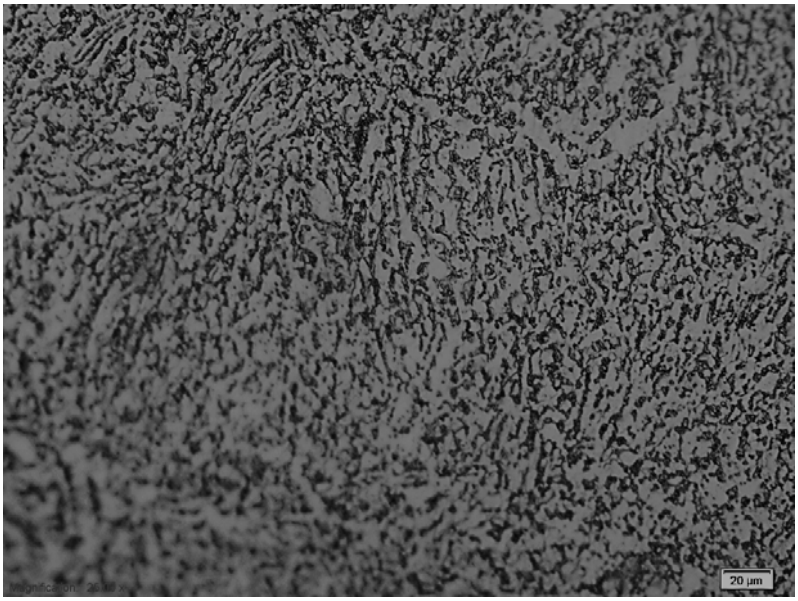

(a)

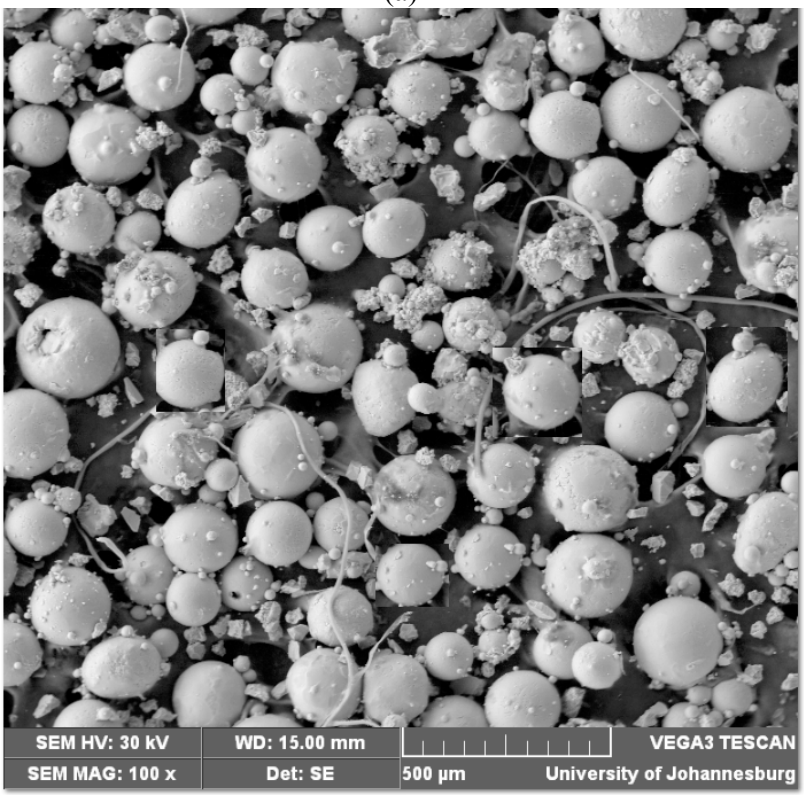

(b)

Figure 2. The micrograph of (a) Ti6Al4V substrate (b) Ti6Al4V powder.

The morphology of the Ti6Al4V powder shown in Figure 2 (b) is spherical in shape because of the gas atomization process used in producing the powder. Spherical shaped powders are more favoured for additive manufacturing process, [29] because it enables proper absorption of the laser energy. The microstructures of the samples produced at scanning speed of 0.02 m/s and 0.12 m/s and at powder flow rate of 2.88 g/min are shown in Figure 3. The microstructure of the sample produced at scanning speed of 0.02 m/s and powder flow rate of 2.88 g/min consists of thick lath of Widmanstätten (basket woven) alpha grains structure as shown in Figure 3 (a) and 3 (b). The microstructure consists of thick lath of Widmanstätten (basket woven) alpha grains structure. The reason for this type of microstructure is that the cooling rate was very slow. Slow solidification and slow cooling rate are associated with large melt-pool that is resulted when the scanning speed is low. At low scanning speed, the laser-material-interaction time is high which gives more time for the melting of the surface of the substrate and the deposited powder which resulted in large melt-pool. Large melt-pool takes longer to solidify and cool down thereby promoting the formation of Widmanstätten alpha grains structure. A thicker lath of this Widmanstätten alpha is observed at this very low scanning speed which is seen to reduce as the scanning speed was increased. The micrograph shown in Figure 3 (b) is that of the sample produced at a scanning speed of 0.12 m/s and powder flow rate of 2.88 g/min. The microstructure shows the presence of martensitic grain structure. The martensitic alpha was formed as a result of rapid cooling rate that occur when the scanning speed is high. At high scanning speed, the laser material interaction time is small and the melt pool produced at this high scanning speed is also small because there was less time for the laser to melt the surface of the substrate ass well as the deposited powder.

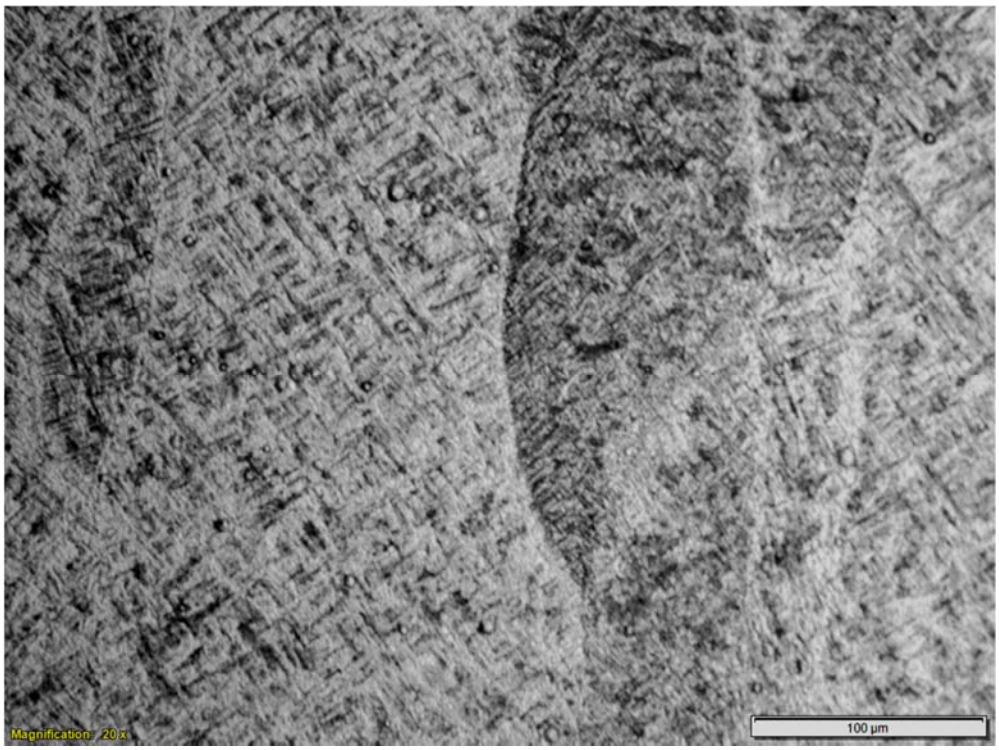

(a)

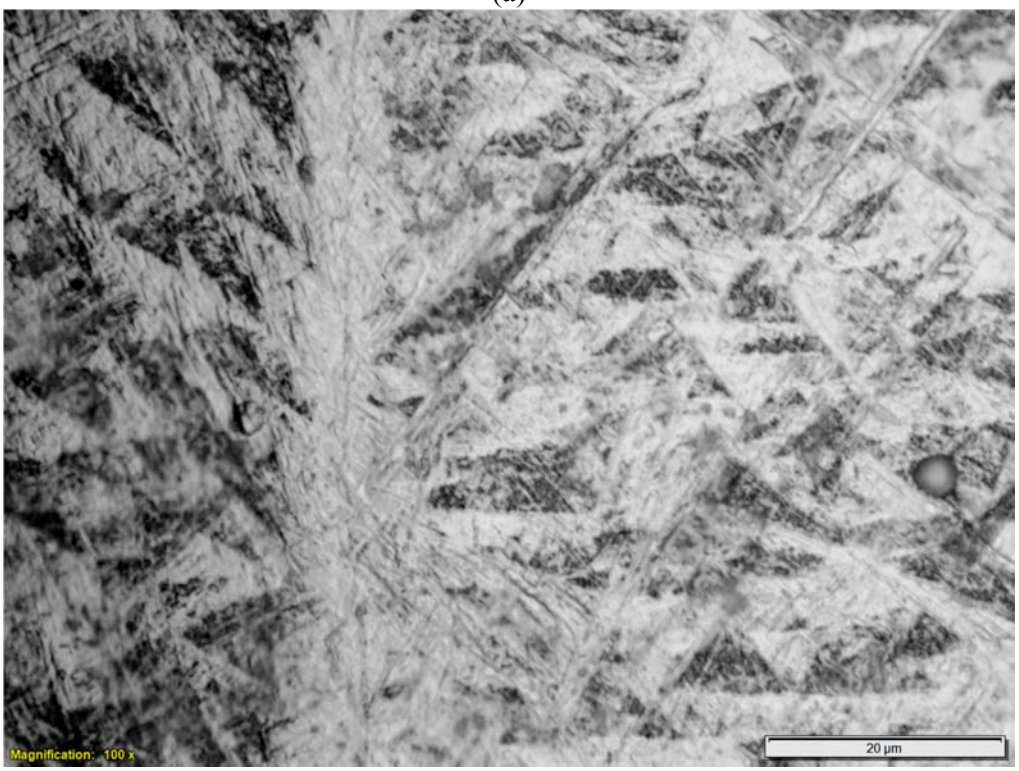

(b)

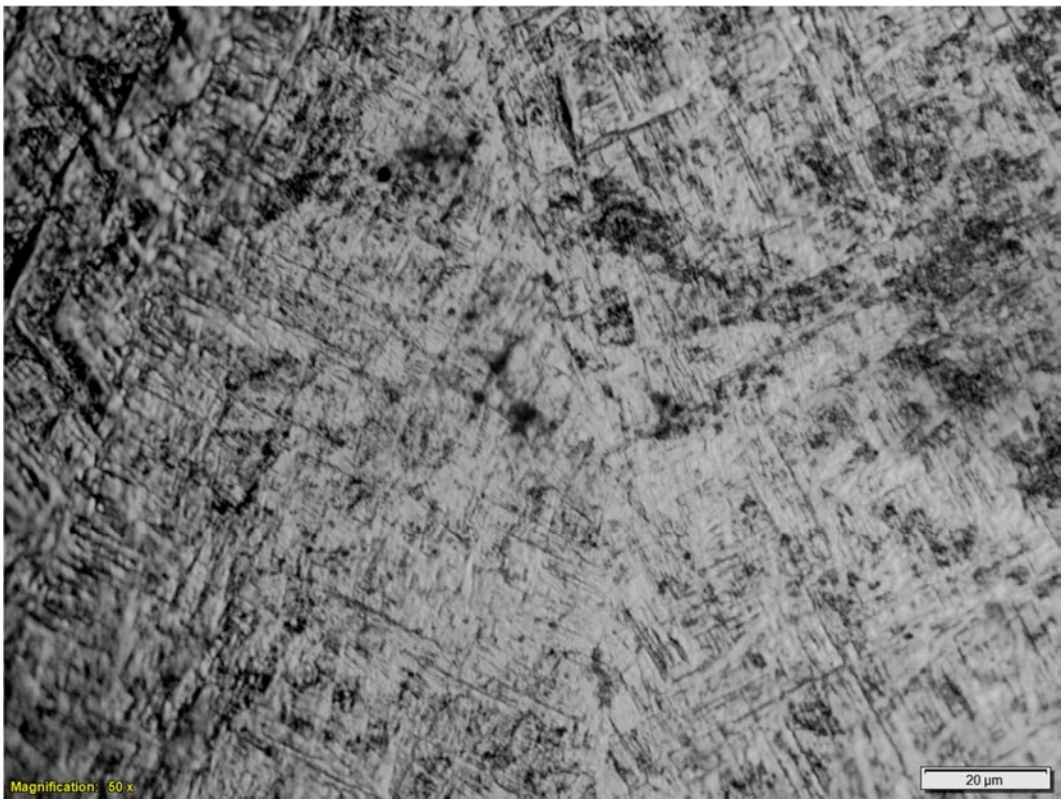

(c)

Figure 3. The micrographs showing the microstructure of samples produced at (a) scanning speed of 0.02 m/s and powder flow rate of 2.88 g/min (b) 3(a) at higher magnification (c) scanning speed of 0.12 m/s and powder flow rate of 2.88 g/min

This is what caused the solidification and the cooling rate to be faster which favors the formation of the martensitic alpha grains observed at this high scanning speed.

The effect of the powder flow rate on the microstructure is observed to be similar to those produced with varying scanning speed. At low powder flow rate, the delivered powder into the melt-pool created by the laser beam on the substrate is low and effective melting took place. The melt-pool created is large because the available laser power is large and the delivered powder is small which

resulted in more melting of the surface of the substrate. Large melt-pool solidifies and cools down slowly which supports the formation of the fine Widmanstätten alpha seen in Figure 4 (a). The mixture of Widmanstätten alpha and martensitic alpha grains are seen at high powder flow rate as shown in Figure 4 (b). At high powder flow rate, the large available powder for melting does not permit large melting of the substrate materials to occur because the large percentage of the available laser power is consumed by the delivered powder. which usually results in the creation of moderate melt-pool size? Moderate melt-pool cause the solidification and the cooling rate to promote the formation of both the Widmanstätten alpha and martensitic alpha grains to be formed as seen in Figure 4 (b). These microstructures are seen to have a direct relationship with the microhardness measured on these samples. The microhardness indentation on the sample at a scanning speed of 0.04 m/s and powder flow rate of 2.88 g/min is shown in Figure 5.

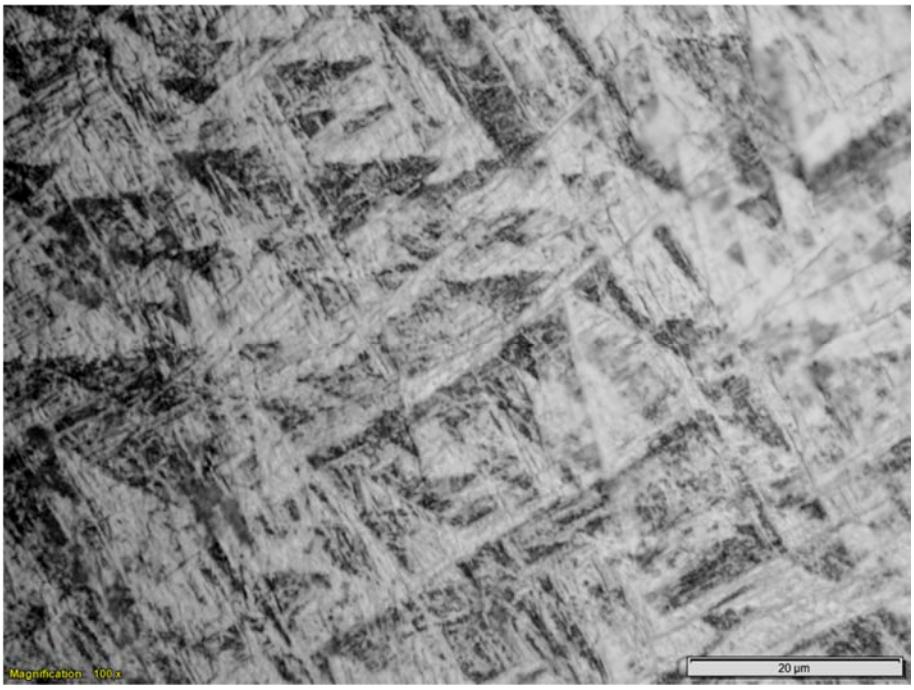

(a)

(a)

Figure 4 the micrographs showing the microstructure of samples produced at (a) scanning speed of 0.06 m/s and powder flow rate of 0.72 g/min (b) scanning speed of 0.06 m/s and powder flow rate of 6.48 g/min

The graph of microhardness against the scanning speed presented in Figure 6 (a) shows that the microhardness increased linearly as the scanning speed was increased. This can be correlated to the microstructures that were described above. The low microhardness obtained at low scanning speed is as a result of the formation of the Widmanstätten alpha grains structure which is soft. The martensites seen at higher scanning speed is responsible for the higher microhardness obtained at higher scanning speed. The rapid solidification associated with the small melt pool and high scanning speed is responsible for the formation of the martensitic alpha grain structures produced which is hard.

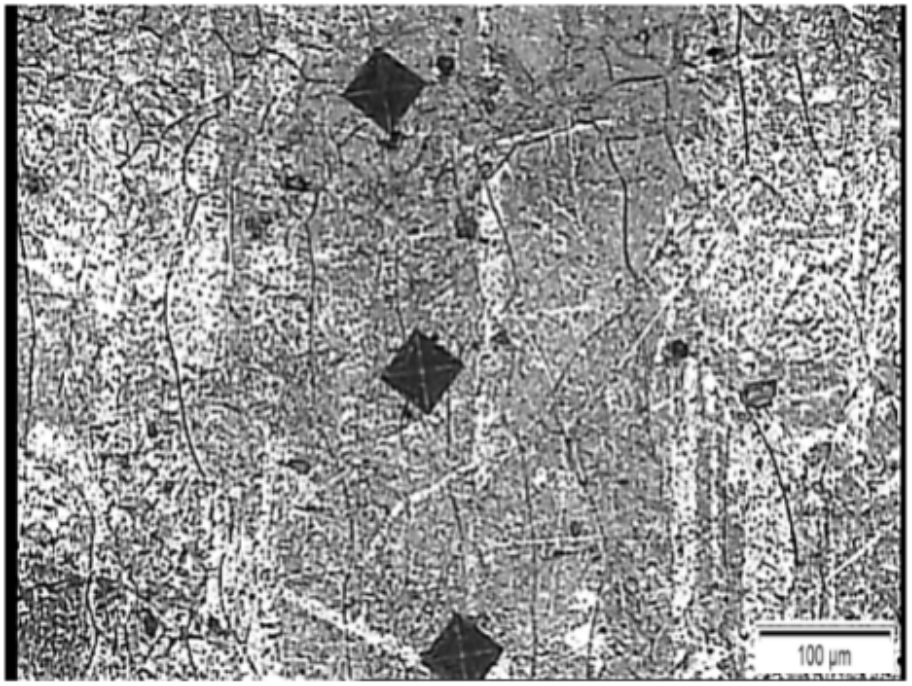

Figure 5. Micrograph of the sample at a scanning speed of 0.04 and powder flow rate of 2.88 g/min

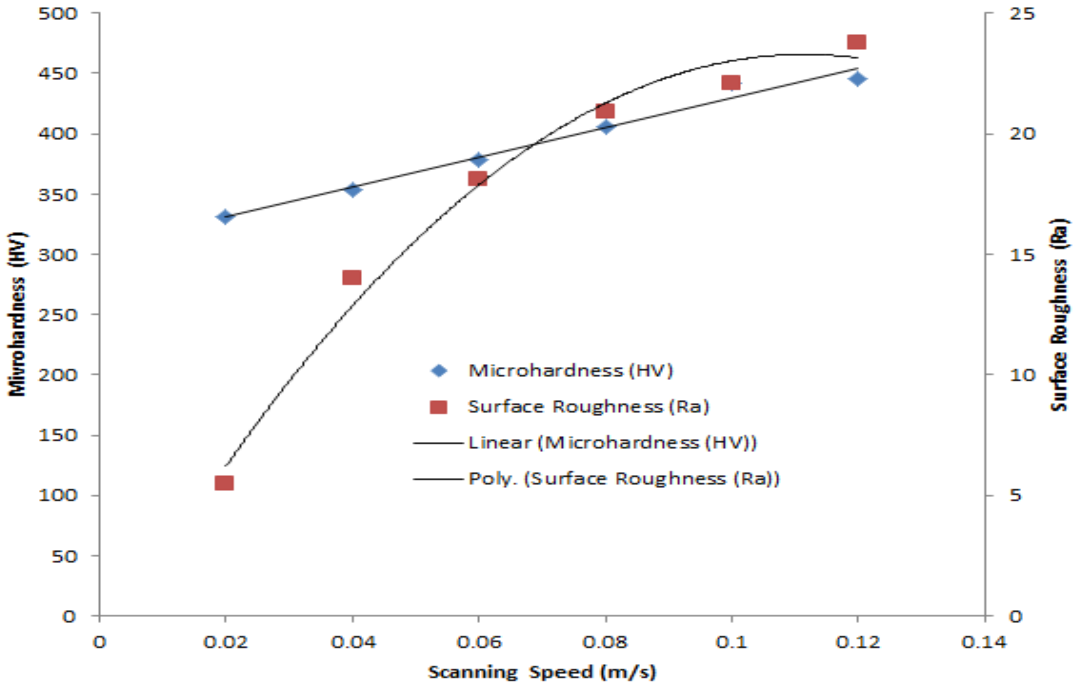

(a)

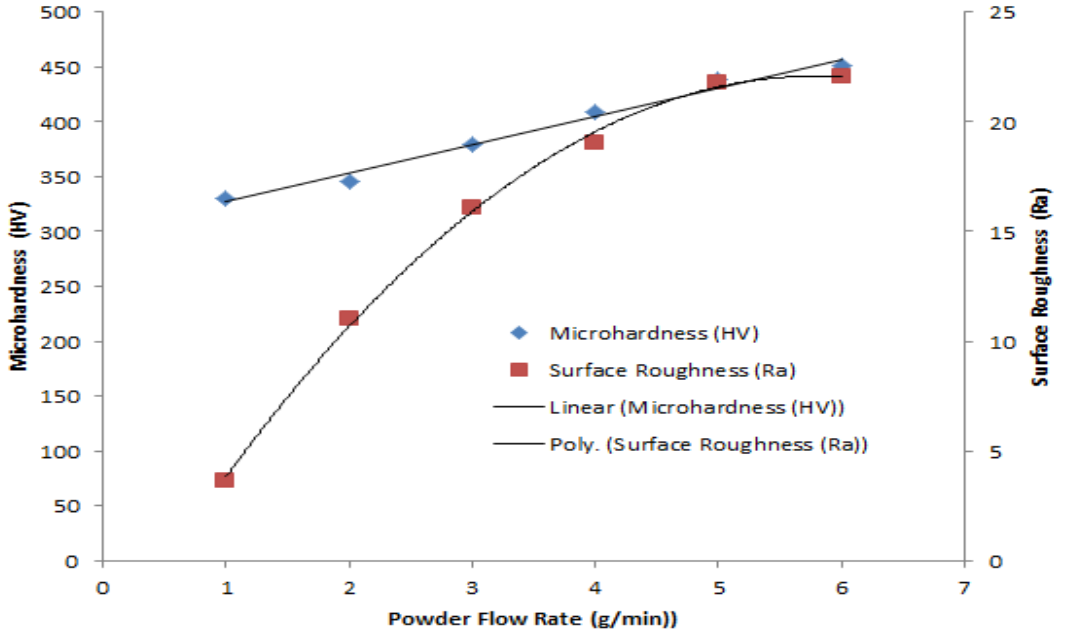

(b)

Figure 6. Graph of microhardness and surface roughness against the (a) scanning speed (b) Powder flow rate.

It can be seen from the graph shown in Figure 6 (a) that the microhardness and the average surface roughness increased as the scanning speed was increased. At low scanning speed, the microhardness was found to be low; this is because of the Widmanstätten alpha grains that are produced at low scanning speed which is characterized by the softness of this grains. As the scanning speed was increased, the microhardness was found to be increased as a result of the presence of the martensitic alpha grains as the scanning speed was increased. Similarly, the average surface roughness was found to increase with the increased in scanning speed as shown in Figure 6 (a) although the surface roughness varied non-lineally with the canning speed. At low scanning speed, there was proper melting of the deposited powder due to the high laser-material-interaction-time and the slow cooling of the melt-pool resulted in the low surface roughness values at the low scanning speed. Conversely, at high scanning speed, the rapid cooling could results in the formation of scales on the surface of the deposited sample which could be responsible for the high average surface roughness values observed at high scanning speed.

From Figure 6 (b), the microhardness was observed to increase with increased in powder flow rate. The low microhardness seen at the low powder flow rate was as a result of the soft Widmanstätten alpha grains structure formed at low powder flow rate due to the large melt pool. The presence of martensitic alpha grains structure which is hard as seen in the microstructure in combination with the Widmanstätten alpha grains structure at high powder flow rate could be responsible for the high microhardness values observed. It could also be as a result of the presence of unmelted powder particles in the deposited sample produced at high powder flow rate. if the available laser power is not enough to properly melt the large deposited powder this could result in higher scanning speed. If this is the case, it is not desirable and there should be limit to which the powder

flow rate should be increased to prevent this from happening. Also, the surface roughness is observed to increase with increase in powder flow rate as shown in Figure 6 (b). At low powder flow rate, the proper melting of the powder and slow solidification as well as slow cooling rate was responsible for the low average surface roughness values obtained. The higher average roughness values seen at high powder flow rate could be as a result of the improper melting of the deposited powder at higher powder flow rate as explained earlier or it could be as a result of scale formation that is associated with rapid cooling of small melt pool. The optimum scanning speed and powder flow rate based on the other fixed processing parameters can be seen in Figure 6 (a) as 0.063 m/s and 2.88 g/min respectively. The reason for selecting these processing parameters as the optimum processing parameters is that, these parameters produce deposit with moderately high microhardness while minimizing the surface roughness value.

5. CONCLUSION

This study examined the influence of the scanning speed and the powder flow rate on the resulting microstructure, microhardness and the surface roughness during laser metal deposition process of Ti6Al4V, an important aerospace alloy. By increasing the scanning speed rate, it was found that the solidification rate was found to be increase that in turn results in the formation of microstructures varying from the soft Widmanstätten alpha grains structure to the hard martensitic alpha grain structures. The microhardness and the average surface roughness were found to increase with the increasing scanning speed which was as a result of these microstructures. Also, the microhardness and the surface roughness were found to increase as the powder flow rate was increased which could be as a result of improper melting of the powder at higher powder flow rate. It can be concluded that the powder flow rate should not be increase too much so as not to result

in improper melting of the deposited sample which could be detrimental to the properties of the deposit. The optimum process parameters for the set of parameters considered in this study is the laser power of 3 kW, scanning speed of 0.063 m/s, the powder flow rate of 2.88 g/min and the gas flow rate of 2 l/min.

ACKNOWLEDGEMENTS

This work was supported by University of Johannesburg research council and the L'OREAL-UNESCO for Women in Science.

REFERERENCES

[1] Scott, J., Gupta, N., Wember, C., Newsom, S., Wohlers, T. and Caffrey, T. (2012*). Additive manufacturing: status and opportunities, Science and Technology Policy Institute*, Available from: https://www.ida.org/stpi/occasionalpapers/papers/AM3D_33012_Final.pdf (Accessed on 11 July 2016)

[2] Allen, J. (2006), An Investigation into the Comparative Costs of Additive Manufacture vs. Machine from Solid for Aero Engine Parts. In Cost Effective Manufacture via Net-Shape Processing, Meeting Proceedings RTO-MP-AVT-139, Paper 17, pp. 1 – 10.

[3] Graf, B., Gumenyuk, A. and Rethmeier, M. (2012). Laser metal deposition as repair technology for stainless steel and Titanium alloys. *Physics Procedia*, 39: 376-381.

[4] Pinkerton, A. J., Wang, W. and Li, L. (2008). Component repair using laser direct metal deposition, *Journal of Engineering Manufacture*, 222: 827-836.

[5] Ermachenko, A. G. Lutfullin, R. Y. and Mulyukov, R. R. (2011). Advanced technologies of processing titanium alloys and their applications in industry, Rev.Adv.Mater. Sci., vol. 29, pp. 68-82.

[6] Donachi, M.J. (2000). *Titanium—A technical guide* , 2nd ed.Metals Park, OH: ASM International.

[7] Lütjering, G. Williams, J.C. (2003). *Titanium*, Springer, Berlin, Germany.

[8] Mahamood, R. M., Akinlabi, E. T., Shukla M. and Pityana, S. (2013a). Laser Metal Deposition of Ti6Al4V: A Study on the Effect of Laser Power on Microstructure and

microhardness. International Multi-conference of Engineering and Computer Science (IMECS 2013), March 2013. 994-999.
[9] Bontha, S. (2006). *The effect of process variables on microstructure in laser-deposited materials,* PhD thesis, Mechanical Engineering, Wright State University.

[10] Brandl, E., Michailov, V., Viehweger, B., Leyens, C., (2011). Deposition of Ti–Al–4V using laser and wire, part I: Microstructural properties of single beads, *Surface & Coatings Technology*, 206, 1120–1129.

[11] Mahamood, R. M. and Akinlabi, E.T. (2015), Process Parameters Optimization for Material Deposition Efficiency in Laser Metal Deposited Titanium Alloy, Lasers in Manufacturing and Materials Processing, DOI 10.1007/s40516-015-0020-5

[12] Mahamood, R. M., Akinlabi, E. T., Shukla M. and Pityana, S. (2014). Characterization of Laser Deposited Ti6A4V/TiC Composite. Lasers in Engineering, 29(3-4), 197-213.

[13] Mahamood, R. M. and Akinlabi, E.T. (2015), Effect of laser power and powder flow rate on the wear resistance behaviour of laser metal deposited TiC/Ti6Al4V composites, *Materials Today: Proceedings*, *Volume 2, Issues 4–5*, *2015*, *Pages 2679-2686*.
[14] Gao, S.Y.; Zhang, Y.Z.; Shi, L.K.; Du, B.L.; Xi, M.Z.; Ji, H.Z. (2007). Research on laser direct deposition process of Ti-6Al-4V alloy. Acta Metallurgica Sinica (English Letters) 20, 171–180.

[15] Krantz, D.; Nasla, S.; Byrne, J.; Rosenberger, B. (2001). On-demand spares fabrication during space missions using laser direct metal deposition, USA: AIP.

[16] Mahamood, R. M., Akinlabi, E. T., Shukla M. and Pityana, S. (2013). Characterizing the Effect of Laser Power Density on Microstructure, Microhardness and Surface Finish of Laser Deposited Titanium Alloy. Journal of Manufacturing Science and Engineering, 135(6), doi:10.1115/1.4025737.

[17] Mahamood, R. M., Akinlabi E. T. and Akinlabi, S. A. (2014a). Laser Power and scanning speed influence on the Mechanical property of laser metal deposited Titanium-alloy, Lasers in Manufacturing and Materials Processing, Volume 2, Issue 1, pp. 43-55.

[18] Ng, G. K. L., Jarfors, A. E. W., Bi, G. and Zheng, H. Y. (2009). Porosity formation and gas bubble retention in laser metal deposition. Applied Physics A, 97, 641–649.

[19] Pityana, S., Mahamood, R. M., Akinlabi, E. T., and Shukla M. (2013). Gas flow rate and powder flow rate effect on properties of laser metal deposited Ti6Al4V. 2013 International Multi-conference of Engineering and Computer Science (IMECS 2013), March 2013. 848-851.

[20] Akinlabi, E. T., Mahamood, R. M., Shukla M. and Pityana, S. (2012). Effect of Scanning Speed on Material Efficiency of Laser Metal Deposited Ti6Al4V. World Academy of Science and Technology, Paris 2012 .vol.6, 58-62

[21] Mahamood, R. M. and Akinlabi, E.T. (2015), Effect of Processing Parameters on Wear Resistance Property of Laser Material Deposited Titanium -Alloy Composite, Journal of Optoelectronics and Advanced Materials (JOAM), Vol. 17, No. 9-10, Pp. 1348 - 1360.

[22] Mahamood, R. M. and Akinlabi, E.T. (2015), Laser metal deposition of functionally graded Ti6Al4V/TiC, Materials & Design, Volume 84, pp. 402-410, ISSN 0264-1275, http://dx.doi.org/10.1016/j.matdes.2015.06.135. (http://www.sciencedirect.com/science/article/pii/S0264127515300265).

[23] Mahamood, R. M. and Akinlabi, E.T. (2015), Effect of laser power and powder flow rate on the wear resistance behaviour of laser metal deposited TiC/Ti6Al4V composites, *Materials Today: Proceedings*, *Volume 2, Issues 4–5*, *2015*, *Pages 2679-2686*.

[24] Mahamood, R. M. and Akinlabi, E.T. (2016), Process Parameters Optimization for Material Deposition Efficiency in Laser Metal Deposited Titanium Alloy, Lasers in Manufacturing and Materials Processing, 3 (1), 9-21, DOI 10.1007/s40516-015-0020-5

[25] Berkmanns, J. and Faerber, M. (2010). *Laser basics, BOC.* Available from: https://boc.com.au/boc_sp/downloads/gas_brochures/BOC_216121_Laser%20Basics_v7.pdf, (Accessed on 25 July 2016).

[26] BS EN ISO 4288:1998, (1998). Geometric product specification (GPS). Surface texture. Profile method: Rules and procedures for the assessment of surface texture, BSI.

[27] E3−11. (2011). Standard Guide for Preparation of Metallographic Specimens, ASTM international Book of Standards, 03 (2011) 01, doi: 10.1520/E0003-11.

[28] ASTM E92 - 16. (2016). Standard Test Method for Vickers Hardness and Knoop hardness of metallic Materials, ASTM International Book of Standards, 03 (01), doi: 10.1520/E0092-16.

[29] Schade, C. T., Murphy T. F. and Walton, C. (2014). Development of Atomized Powders for Additive Manufacturing, Powder Metallurgy Word Congress, (2014). Accessed on 2nd July 2014 available at: http://www.gkn.com/hoeganaes/media/Tech%20Library/Schade-Atomized%20Powders%20for%20Additive%20Manufacturing%20%281%29.pdf